# Form factor in $K^+ \to \pi^+\pi^0\gamma$: interference versus direct emission

Luigi Cappiello and Giancarlo D'Ambrosio
*INFN – Sezione di Napoli*
and
*Dipartimento di Scienze Fisiche,*
*Università di Napoli "Federico II"*
*Via Cintia, 80126 Napoli, Italy*

(Dated: February 2, 2008)

We analyze the effect of a form factor in the magnetic contribution to $K^+ \to \pi^+\pi^0\gamma$. We emphasize how this can show up experimentally: in particular we try to explore the difference between a possible interference contribution and a form factor in the magnetic part. The form factor used for $K^+ \to \pi^+\pi^0\gamma$ is analogous to the one for $K_L \to \pi^+\pi^-\gamma$, experimentally well established.

PACS numbers: 12.39.-y, 13.25.Es

arXiv:hep-ph/0702292v2 19 Apr 2007

## I. INTRODUCTION

Non-leptonic kaon decays are an important tool to study weak interactions [1, 2, 3, 4, 5, 6, 7]. Radiative non-leptonic kaon decays, such as $K_{L,S} \to \pi^+\pi^-\gamma$ and $K^+ \to \pi^+\pi^0\gamma$ are dominated by long distance contributions. The study of these decays leads to chiral tests and in principle to disentangle the small short distance contribution. This small short distance part may lead also to interesting CP violating observables in the Standard Model (SM) and Beyond (BSM) [8].

$K \to \pi\pi\gamma$ amplitudes contain two types of contributions: inner bremsstrahlung (IB) and direct emission (DE). Due to the pole in the photon energy the IB amplitude is generally enhanced compared to DE; however the IB components of $K_L \to \pi^+\pi^-\gamma$ and $K^+ \to \pi^+\pi^0\gamma$ are suppressed due, respectively, to CP invariance and to the $\Delta I = 1/2$ rule. Then, the DE amplitude of these channels, that are the non-trivial part of these decays, might also be easier to detect. DE contributions can be decomposed into electric (E1,E2) and magnetic (M1,M2) ones [9]. The magnetic contribution to $K_L \to \pi^+\pi^-\gamma$ is accurately measured [10, 11] and a clear and large photon energy dependence has been found.

The question of the presence of the form factor, i.e. the size of vector meson dominance in weak amplitudes, is motivated not only by phenomenological reasons, as in $K_L \to \pi^+\pi^-\gamma$, but it has also theoretical motivations [2]. For instance, it improves the matching of long and short distance contributions [2].

Published data for $K^\pm \to \pi^\pm\pi^0\gamma$ are consistent with a dominant magnetic amplitude and no evidence for E1 transitions [11]. However, preliminary data from NA48/2 at CERN show a non-vanishing interference, due to E1 transitions [12, 13]: the size of this contribution will shed light on $O(p^4)$ chiral perturbation theory ($\chi$PT) counterterm coefficients [1, 14, 15]. The energy dependence of the $K^+ \to \pi^+\pi^0\gamma$ magnetic amplitude has not been tested/observed yet; we think it is important to understand if the form factor in the magnetic contribution affects the determination of the electric contributions: in this paper we complement Ref.[16] with this perspective.

Long ago N. Christ used a particular set of $K^\pm \to \pi^\pm\pi^0\gamma$ Dalitz variables: the photon energy and the charged pion kinetic energy in the kaon rest frame [17]. NA48/2 [12, 13] wants to perform an analysis using these variables too; in the following we give a kinematical distribution in these variables accounting for the $m_{\pi^+} - m_{\pi^0}$ corrections. Furthermore, the results in Ref.[16] considered essentially the central value of branching ratio from E787 [18], $(4.7\pm0.8)\times10^{-6}$. Recent results [13, 19] seem to prefer smaller values, $(2 \sim 3) \times 10^{-6}$; while this is not shocking by itself, it has some impact if we include the form factor as we shall see. We discuss $K \to \pi\pi\gamma$ kinematics and Low theorem in Section 2; in Section 3 we carry out some theoretical-phenomenological considerations on $K \to \pi\pi\gamma$. Numerical results are summarized in Section 4.

## II. KINEMATICS AND LOW THEOREM

The general invariant amplitude of $K \to \pi\pi\gamma$ can be defined as follows [4, 20]

$$A[K(p) \to \pi_1(p_1)\pi_2(p_2)\gamma(q,\epsilon)] = \epsilon^\mu(q) M_\mu(q, p_1, p_2),$$

where $\epsilon_\mu(q)$ is the photon polarization and $M_\mu$ is decomposed into an electric $E$ and a magnetic $M$ amplitudes as

$$M_\mu = \frac{E(z_i)}{m_K^3}[p_1\cdot q p_{2\mu} - p_2\cdot q p_{1\mu}] + \frac{M(z_i)}{m_K^3}\epsilon_{\mu\nu\alpha\beta}p_1^\nu p_2^\alpha q^\beta,$$

with

$$z_i = \frac{q\cdot p_i}{m_K^2},\ (i=1,2),\ \ z_3 = \frac{p\cdot q}{m_K^2},\ \ z_3 = z_1 + z_2. \quad (1)$$

The double differential rate for the unpolarized photon is

$$\frac{\partial^2\Gamma}{\partial z_1 \partial z_2} = \frac{m_K}{(4\pi)^3}\left[|E(z_i)|^2 + |M(z_i)|^2\right] \times \left[z_1 z_2(1-2z_3-r_1^2-r_2^2) - r_1^2 z_2^2 - r_2^2 z_1^2\right], \quad (2)$$

where $r_i = m_{\pi_i}/m_K$. Low theorem establishes a precise relation between radiative and non-radiative amplitudes in the limit of $E_\gamma \to 0$ [9, 21]. Then we can generally write the relation between the bremsstrahlung amplitude, $E_{IB}$, in $K \to \pi\pi\gamma$ decays and the on-shell amplitude, $A(K \to \pi\pi)$:

$$E_{IB}(z_i) \doteq \frac{eA(K\to\pi_1\pi_2)}{m_K z_3}\left(\frac{Q_2}{z_2} - \frac{Q_1}{z_1}\right), \quad (3)$$

where $Q_i$ is the $\pi_i$ charge. Direct emission amplitudes are defined by subtracting this contribution from the total amplitude. In the $K^+$ case

$$E_{IB}(K^+) \ = \ e^{i\delta_2}\left(\frac{3eA_2}{2m_K z_+ z_3}\right) \quad (4)$$

where $A(K^+ \to \pi^+\pi^0) = \frac{3}{2}A_2 e^{i\delta_2}$ and $z_+$ refers to the charged pion. Using the experimental value for $B(K^+ \to \pi^+\pi^0)$ we obtain the branching ratios for the Inner Bremsstrahlung shown in TAB. I.

| $T_c^*$-range in MeV | $B(K^+ \to \pi^+\pi^0\gamma)_{\rm IB}$ |
|---|---|
| $[55, 90]$ | $(2.61)\times10^{-4}$ |
| $[0, 80]$ | $(1.84)\times10^{-4}$ |

TABLE I: Inner Bremsstrahlung

In $K_L \to \pi^+\pi^-\gamma$, the most common variables are: *i)* the photon energy in the kaon rest frame $E_\gamma^*$, and *ii)* the angle $\theta$ between the photon and $\pi^+$ momenta in the di-pion rest frame. The relations between $E_\gamma^*$, $\theta$ and the $z_i$ are:

$$z_3 = \frac{E_\gamma^*}{m_K}, \quad z_\pm = \frac{E_\gamma^*}{2m_K}(1 \mp \beta\cos\theta), \quad (5)$$

where $\beta = \sqrt{1 - 4m_\pi^2/(m_K^2 - 2m_K E_\gamma^*)}$. Then the differential rate is

$$\frac{\partial^2\Gamma}{\partial E_\gamma^* \partial\cos\theta} = \frac{(E_\gamma^*)^3\beta^3}{512\pi^3 m_K^3}\left(1 - \frac{2E_\gamma^*}{m_K}\right)\sin^2\theta \ (|E|^2 + |M|^2). \quad (6)$$

Since three photons will be detected in the $K^+ \to \pi^+\pi^0\gamma$ measurement, it is very useful to study the differential rate as a function of: *i)* the charged pion kinetic energy in the $K^+$ rest frame $T_c^*$, and *ii)* $W^2 = (q\cdot p_K)(q\cdot p_+)/(m_{\pi^+}^2 m_K^2)$ [9]. These two variables are related to the $z_i$ by

$$z_0 = \frac{m_K^2 + m_{\pi^+}^2 - m_{\pi^0}^2 - 2m_K m_{\pi^+} - 2m_K T_c^*}{2m_K^2},$$
$$z_3 z_+ = \frac{m_{\pi^+}^2}{m_K^2}W^2. \quad (7)$$

The advantage of these variables is that, under the assumption of constant $E_{DE}$ and $M_{DE}$, one can easily disentangle the different contributions of the IB, DE amplitudes, and interference term between IB and DE

$$\frac{\partial^2\Gamma}{\partial T_c^* \partial W^2} = \frac{\partial^2\Gamma_{IB}}{\partial T_c^* \partial W^2}\left[1 + \frac{m_{\pi^+}^2}{m_K}2Re\left(\frac{E_{DE}}{e\mathcal{A}}\right)W^2 + \frac{m_{\pi^+}^4}{m_K^2}\left(\left|\frac{E_{DE}}{e\mathcal{A}}\right|^2 + \left|\frac{M_{DE}}{e\mathcal{A}}\right|^2\right)W^4\right], \quad (8)$$

where

$$\mathcal{A} = A(K^+ \to \pi^+\pi^0). \quad (9)$$

### A. Kinematics in Christ's variables $T_c^*$ and $E_\gamma^*$

Motivated by the upcoming NA48 measurements we have also studied the Dalitz plot distributions in the kinematical variables $T_c^*$ and the photon energy in the kaon rest frame, $E_\gamma^*$. In this way we extend the work by N. Christ [17] by including the terms proportional to $m_{\pi^+} - m_{\pi^0}$; in these variables the double differential rate for $K^+ \to \pi^+\pi^0\gamma$ is written as

$$\frac{\partial^2\Gamma}{\partial T_c^* \partial E_\gamma^*} = \frac{\partial^2\Gamma_{IB}}{\partial T_c^* \partial E_\gamma^*}\left[\ 1 \ + \ 2Re\left(\frac{E_{DE}}{e\mathcal{A}}\right)\left(\frac{m_K}{2} - E_0 - \frac{\delta\mu^2}{2m_K}\right)\frac{E_\gamma^*}{m_K} + \left(\left|\frac{E_{DE}}{e\mathcal{A}}\right|^2 + \left|\frac{M_{DE}}{e\mathcal{A}}\right|^2\right)\left(\frac{m_K}{2} - E_0 - \frac{\delta\mu^2}{2m_K}\right)^2\frac{E_\gamma^{*2}}{m_K^2}\right], \quad (10)$$

where $E_0$ is the $\pi^0$-energy,

$$\delta\mu^2 = m_{\pi^+}^2 - m_{\pi^0}^2$$

and the Inner Bremsstrahlung differential rate is written in terms of angle, $\theta$, between the $\pi^+$ and $\gamma$ momenta in the kaon rest frame

$$\cos\theta \ = \ \frac{m_K^2 - 2\,m_K E_\gamma^* + 2\,(T_c^* + m_{\pi^+})(E_\gamma^* - m_K) + \delta\mu^2}{2\,p_{\pi^+}^*\,E_\gamma^*}$$

$$p_{\pi^+}^* = \sqrt{T_c^*(T_c^* + 2m_{\pi^+})},$$

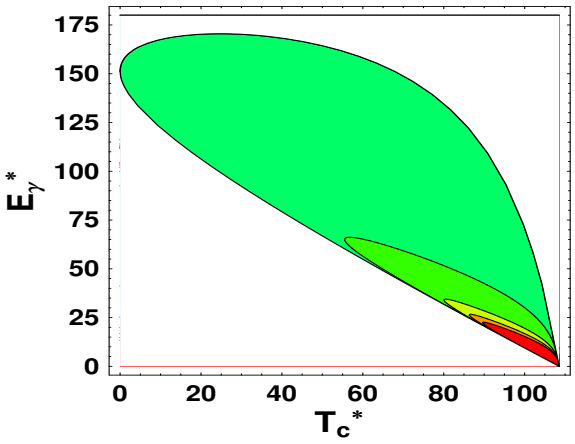


FIG. 1: Dalitz plot of Christ's variables $T_c^*$ and $E_\gamma^*$ and contour plot of the Inner Bremsstrahlung amplitude: the right corner (in red) has a greater density.

$$\frac{\partial^2\Gamma_{IB}}{\partial T_c^*\partial E_\gamma^*}=\frac{\alpha}{(4\pi)^2}\frac{{p_+^*}^2}{m_K^3}\sin^2\theta\frac{|\mathcal{A}|^2}{\left(\frac{m_K}{2}-E_0-\frac{\delta\mu^2}{2m_K}\right)^2}.$$

It is possible to pass from eq.(10) to eq.(8) through

$$W^2=\frac{E_\gamma^*}{m_{\pi^+}^2}(E_\gamma^*+T_c^*+m_{\pi^+}-\frac{m_K}{2}-\frac{\delta\mu^2}{2m_K}).$$

A contour plot of the IB amplitude in the Dalitz plot of Christ's variables $T_c^*$ and $E_\gamma^*$ is shown in FIG.1. After integrating eq.(10) on $E_\gamma^*$, one obtains $(E_c^*=T_c^*+m_{\pi^+})$

$$\frac{d\Gamma}{dT_c^*}=\frac{\alpha\,|\mathcal{A}|^2}{(2\pi)^2}\left\{\frac{2\left[\frac{E_c^*}{m_K}\log(\frac{E_c^*+p_+^*}{m_{\pi^+}})-\frac{p_+^*}{m_K}\right]}{m_K\left(m_K-2E_c^*+\frac{\delta\mu^2}{m_K}\right)}\right.$$

$$+Re\left(\frac{E_{DE}}{e\mathcal{A}}\right)\frac{m_K-2E_c^*+\frac{\delta\mu^2}{m_K}}{2m_K^2}\left[\frac{1}{2}\left(1-\frac{m_{\pi^+}^2}{m_K^2}\right)\cdot\right.$$

$$\left.\log\left(\frac{m_K-E_c^*+p_+^*}{m_K-E_c^*-p_+^*}\right)-\frac{m_{\pi^+}^2}{m_K^2}\log\left(\frac{E_c^*+p_+^*}{m_{\pi^+}}\right)-\frac{p_+^*}{m_K}\right]$$

$$\left.+\left(\left|\frac{E_{DE}}{e\mathcal{A}}\right|^2+\left|\frac{M_{DE}}{e\mathcal{A}}\right|^2\right)\frac{{p_+^*}^3\left(m_K-2E_c^*+\frac{\delta\mu^2}{m_K}\right)^3}{24m_K^2\left((m_K-E_c^*)^2-{p_+^*}^2\right)^2}\right\}$$

## III. EXPERIMENTAL STATUS AND THEORETICAL PREDICTIONS

Electric and magnetic dipole (E1 and M1) transitions appear already at $\mathcal{O}(p^4)$ [14, 15]. Since $K^+$ is not a CP eigenstate, M1 and E1 transitions are CP-allowed in $K^+$, while for $K_L$, CP-symmetry allows M1 transitions and inhibits E1 transitions. The $\mathcal{O}(p^4)$ contributions to $K^+$ electric transitions can be parametrized as

$$E_1(K^+) \;=\; -e^{i\delta_c}\frac{eG_8m_K^3}{8\pi^2F_\pi}N_{E_1}^{(4)}, \qquad (11)$$

where $G_8=9\cdot10^{-6}$ GeV$^{-2}$ is obtained from the $\Delta I=1/2$ contribution to $K_S\to\pi\pi$ at $\mathcal{O}(p^2)$ and $N_{E_1}^{(4)}$ is the relevant $\mathcal{O}(p^4)$ weak counterterm combination [14, 15, 20]

$$N_{E_1}^{(4)} \;=\; (4\pi)^2\left[N_{14}-N_{15}-N_{16}-N_{17}\right]$$
$$\stackrel{FM}{=}\; -k_f\frac{8\pi^2F_\pi^2}{m_V^2}=-(0.4\div1). \qquad (12)$$

The second line is the theoretical prediction based on the factorization model (FM) [1, 14, 15, 20, 22] parametrized by the a coefficient $k_f$. From naïve dimensional analysis (NDA) we expect $N_{E_1}^{(4)}$ of order one; in fact this value is expected from VMD and factorization [1, 15]. The sign in (11) and (12) leads to a constructive interference among $E_1$ and $E_{IB}$ [20] but *so far there is no experimental evidence of such interference*, up to the new NA48 result [13], as we shall see.

Actually, the present bounds [18, 19] are very close to the theoretical predictions [1, 14, 15]; in TAB. II we report instead the results for a destructive interference, $N_{E_1}^{(4)}=0.4$, as reported by NA48 [13]. The interference term scales linearly with $N_{E_1}^{(4)}$, then branchings for different $N_{E_1}^{(4)}$ values are easily obtained. The same counterterm coefficient, $N_{E_1}^{(4)}$, appears in the DE component of $K_S\to\pi^+\pi^-\gamma$ [20, 23], however the present experimental bound [24] is not at the level to compete with the one from $K^+\to\pi^+\pi^0\gamma$.

No $E1$ (CP violating) transitions for $K_L$ have been observed yet [10]; while the magnetic contributions, $M1$ is responsible for the observed $\mathrm{B}(K_L\to\pi^+\pi^-\gamma)_{DE}$. The leading order magnetic amplitude, $M(z_i)$, to eq. (1), starts at $O(p^4)$ [4, 21]

$$M_L^{(4)}=\frac{eG_8m_K^3}{2\pi^2F}(a_2+2a_4), \qquad (13)$$

$$M_+^{(4)}=-\frac{eG_8m_K^3}{4\pi^2F}[2+3(2a_3-a_2)]. \qquad (14)$$

The subscripts $L$ and $+$ denote $K_L\to\pi^+\pi^-\gamma$ and $K^+\to\pi^+\pi^0\gamma$ respectively. The $a_i$'s parts of the above amplitudes come from the local weak lagrangian $\mathcal{L}_4^{\Delta S=1}$ and are expected of order one [4, 25]; these are also called direct contributions. They were originally derived using the factorized

form, current-current, of the weak chiral lagrangian with one current $\mathcal{O}(p^3)$ from the WZW lagrangian and the other current from the usual $\mathcal{O}(p)$ current [25]. Later it was found that also vectors and axials (VMD) were contributing to these coefficients ($a_i$'s) [15]. The factor "2"in (14) is the contribution from the $K^+ \to$ "$\pi^+$"$\to \pi^+\pi^0\gamma$, where we have first a pure weak transition and then a Wess-Zumino-Witten one and thus it is completely predicted (indirect contribution). There are too many $a_i$'s to be fixed phenomenologically and possibly large $\mathcal{O}(p^6)$ corrections to $K_L \to \pi^+\pi^-\gamma$ in (13) from $\eta'$-exchange.

An interesting progress to the understanding of these decays has been driven by KTeV; in order to fit the $K_L \to \pi^+\pi^-\gamma$ data showing a clear photon energy dependence in the magnetic term, $M(z_i)$, KTeV has used a linear fit, a quadratic fit or a pole fit of the form

$$M_L = e\,|h_M| \left( \frac{b}{1 - \frac{m_K^2}{m_V^2} + \frac{2m_K}{m_V^2} E_\gamma^*} + 1 \right). \quad (15)$$

Interestingly, data prefer this pole fit to linear and quadratic fit [10]. The rate and the photon energy spectrum fix $|h_M| = (9.4 \pm 0.8) \cdot 10^{-7}$ and $b = -1.243 \pm 0.033$ [10]. This phenomenological description has been comforted by NA48 [26] and KTeV [27] in the channel $K_L \to \pi^+\pi^- e^+ e^-$. Comparison of (15) with (13) leads to the following theoretical consequences: i) the value of $h_M$ fixes the size of the $a_i$'s: $\sim \mathcal{O}(1)$ and ii) the presence of a relatively large component, $b$, with form factor tells us that VMD plays a major rôle in these coefficients. The usual vector formulation, "$V^\mu$", is very successful to this description: there are vector and axial contributions to the $a_i$'s [15]. However the tensor formulation of the vectors, "$V^{\mu\nu}$", very successful in the strong sector, does not have any vector contributions to the $a_i$'s [14, 16]. The lack of vector contributions to the $a_i$'s and possible large $\mathcal{O}(p^6)$ contribution to (13) from $\eta'$-exchange does not explain the observed large form factor in (15) and puts tension in the chiral expansion with large $\mathcal{O}(p^6)$ and small $\mathcal{O}(p^4)$ contributions [4]. Actually, in Ref. [28] it was already shown that while the odd-parity couplings to $V \to P\gamma$ decays, relevant to the anomalous $K \to \pi\pi\gamma$ decays, had the proper QCD behaviour if we use the usual vector formulation, "$V^\mu$", this was not the case if we use the tensor formulation of the vectors, "$V^{\mu\nu}$". As a result we believe in the large VMD contribution to the $a_i$'s.

We show in TAB. II an updated $K^+ \to \pi^+\pi^0\gamma$ experimental and theoretical situation. We write in the first two lines the PDG 06 value along with its most precise measurement, BNL E787; in the next two lines two subsequent measurements, KEK-E470 and NA48/2, that as we can see, point towards a smaller value of the branching ratio. All these values are obtained with vanishing interference. Also to compare NA48/2 with other experiments we extrapolated the NA48/2 value, obtained in the kinematical range $0 \le T_c^* \le 80$ MeV, to the kinematical range $55 \le T_c^* \le 90$ MeV assuming a constant magnetic term. Interestingly NA48/2 has also done the analysis to determine simultaneously both the interference and the direct emission contributions [13]; we show in TAB. II this NA48/2 analysis show-

Experimental status

| REFS. | $B(K^+ \to \pi^+\pi^0\gamma)_{\rm DE}$ $T_c^* \in [55, 90]$ |
|---|---|
| BNL E787 [18] | $(4.7\pm0.9)\times10^{-6}$ |
| PDG 06 [11] | $(4.4\pm0.7)\times10^{-6}$ |
| KEK-E470 [19] | $(3.8\pm0.8\pm0.7)\times10^{-6}$ |
| NA48/2 [13] | $(2.22\pm0.13\pm0.05)\times10^{-6}$ |

| NA48/2 analysis [13] | $T_c^* \in [0, 80]$ MeV |
|---|---|
| $B(K^+ \to \pi^+\pi^0\gamma)^{\rm INT}$ | $(-4.91\pm2.00)\times10^{-6}$ |
| $B(K^+ \to \pi^+\pi^0\gamma)^{\rm DE}$ | $(6.16\pm0.79)\times10^{-6}$ |

Theory predictions

| $T_c^*$-range in MeV | $B(K^+ \to \pi^+\pi^0\gamma)_{\rm INT}^{N_{E_1}^{(4)}=0.4}$ |
|---|---|
| $[55, 90]$ | $-(3.52)\times10^{-6}$ |
| $[0, 80]$ | $-(4.70)\times10^{-6}$ |

| $T_c^*$-range in MeV | $B(K^+ \to \pi^+\pi^0\gamma)_{\rm DE}^{a_i=0}$ |
|---|---|
| $[55, 90]$ | $(3.55)\times10^{-6}$ |
| $[0, 80]$ | $(6.57)\times10^{-6}$ |

TABLE II: Experimental and theoretical status
The table shows in the first two lines the PDG 06 value along with its most precise measurement, BNL E787 and in the next two lines two subsequent measurements, KEK-E470 and NA48/2, pointing towards a smaller value of the branching ratio. All these values are obtained with vanishing interference. To compare NA48/2 with other experiments we extrapolated the NA48/2 value, obtained in the kinematical range $0 \le T_c^* \le 80$ MeV, to the kinematical range $55 \le T_c^* \le 90$ MeV, assuming a constant magnetic term. We report in the fifth and sixth row, the interference and the direct emission contributions determined simultaneously by NA48/2 [13]. The INT theoretical branching ratio with a value of the weak counterterm combination in eq. (12) so to match the NA48/2 result, $N_{E_1}^{(4)} = 0.4$, is then shown. For comparison the DE theoretical branching ratios obtained with $a_i = 0$ are reported in the last rows.

ing non-vanishing values for both the interference and the direct emission contributions.

We also show in TAB. II for comparison some theoretical predictions for the interference term and the direct emission term. Regarding the interference term we use a specific value of the weak counterterm combination in eq. (12): $N_{E_1}^{(4)} = 0.4$, so to match the NA48/2 result. Regarding the DE contribution we take as comparison the $a_i = 0$.

Following Ref. [16] a correlated analysis of the $K^+ \to \pi^+\pi^0\gamma$ and $K_L \to \pi^+\pi^-\gamma$ decays can be performed. VMD and phenomenology, i.e. eq. (15), imply the following decomposition:

$$M_+(z_i) = M_+^{\rm pole} + M_+^{\rm const.} \tag{16}$$

It is interesting that all the weak couplings involving vectors, and consequently $M_+$ and $M_L^{\rm VMD}$, may be written in terms of only one coupling, $\eta_V$ [15]. Thus we parametrize all our ignorance in $M_{\rm pole}^+$ with $\eta_V$:

$$M_+^{\rm pole}(z_i) = -\frac{eG_8m_K^3}{4\pi^2F}r_V\left(\frac{1-2z_3+\frac{m_V^2}{m_K^2}\eta_V}{1-\frac{m_K^2}{m_V^2}+\frac{2m_K^2}{m_V^2}z_3}+\right.$$
$$\left.\frac{2z_+-\frac{m_V^2}{2m_K^2}\eta_V}{1-\frac{2m_K^2}{m_V^2}z_+}+\frac{2z_0+\frac{m_V^2}{m_K^2}\eta_V}{1-\frac{2m_K^2}{m_V^2}z_0}\right), \tag{17}$$

where

$$r_V = \frac{32\sqrt{2}\pi^2 f_V h_V m_K^2}{3m_V^2}, \tag{18}$$

is determined by the VMD couplings [4, 15] $f_V = 0.2$ and $h_V = 0.037$, well known phenomenologically. The rest is written as a constant contribution,

$$M_+^{\rm const.} = -\frac{eG_8m_K^3}{4\pi^2F}A^+, \tag{19}$$

where the parameter

$$A^+ = 2+3(2a_3-a_2)_{\rm non-VMD}+\text{ other contributions.}$$

must be determined phenomenologically. $(2a_3 - a_2)_{\rm non-VMD}$ is a non-VMD contribution to $M^+$; thus the experimental $B(K^+ \to \pi^+\pi^0\gamma)_{DE}$ can be obtained by varying the two unknown constants $(A^+, \eta_V)$. In FIG. 2, we vary respectively $1\sigma$, $2\sigma$ and $3\sigma$ deviations around the BNL E787 result [18] similar to the PDG result in TAB. II. So we can account properly the sensitivity of the $W-$ and $T_c^*-$spectrum from these phenomenological parameters which we will discuss in the next paragraph.

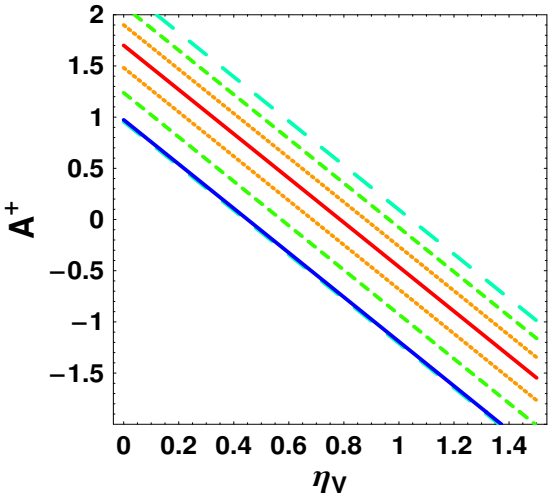


FIG. 2: Values of $A^+$ and $\eta_V$ on the central solid line generate the E787 experimental value of the branching ratio in TAB. II while the other lines are the borders of strips corresponding to $1\sigma$, $2\sigma$ and $3\sigma$ deviation from the E787 central value in TAB. II. As a result the lower solid line corresponds to the central NA48 value in TAB. II. For $\eta_V = 0$ and $A^+ = 2$, the amplitude is dominated by the WZW pole.

In fact, recent data, shown in TAB. II, point towards smaller values of the branching.

NA48, in their preliminary analysis [13], are able to study this decay in a new kinematical region: the charged pion kinetic energy ranges from 0 to 80 MeV; as we can see from FIG. 1, this region is more sensitive to the DE component. Furthermore assuming a **constant** $M(z_i)$ in (1) they find a non-vanishing $E1$-contribution.

This result is very interesting; in particular though the size is comparable to the theoretical expectations in (12) and TAB. II [1, 14, 15], the sign is opposite as discussed before. In the next section we investigate the consequences of the presence of the form factor on this NA48 measurement.

## IV. EFFECT OF THE FORM FACTOR ON THE DIRECT EMISSION AMPLITUDE

The target of the following numerical studies is to understand how to distinguish a constant magnetic term, practically $\eta_V = 0$, from the one with the form factor in eqs. (16) and (17), in FIG. 2. A related question is, as we shall see, if the possible presence of a form factor affects the determination of the interference term or even if the presence of the form factor could mimic the experimental evidence

of the interference term. It is important, we think, to quantify this effect.

Previous experiments were able to study only the kinematical range $T_c^* \in [55, 90]$ MeV [18, 19]; recentely NA48/2 has been able to uncover almost the full range $T_c^* \in [0, 80]$ MeV [13]. The region with small values for $T_c^*$ is more sensitive to DE transitions. Indeed the explicit IB Dalitz plot contour in the $T_c^*$ and $W$ variables generates a plot similar to FIG. 1. Due to the sensitivity of the kinematical distributions from the size of DE branchings we will discuss both possibilities $\mathbf{B_{exp}(E787)}$ and $\mathbf{B_{exp}(NA48)}$ in both kinematical regions.

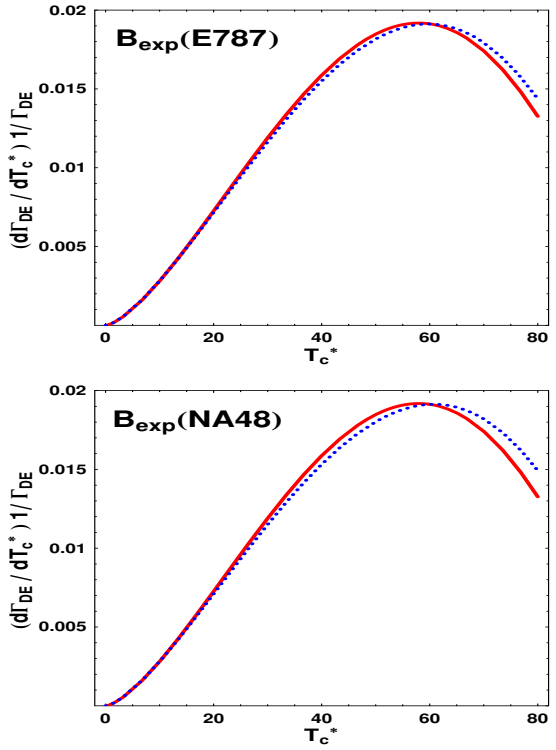


FIG. 3: Normalized $T_c^*$-spectra ($T_c^* \in [0, 80]$ MeV) for the DE magnetic amplitude with the E787 branching ratio [18] in TAB. II (upper plot) and the NA48/2 branching ratio in TAB. II (lower plot). The solid curves correspond to a constant amplitude, the dotted curves to a magnetic form factor with $\eta_V = 1.5$ and corresponding value of $A^+$ on the central (lower) full line of FIG. 2 for the upper (lower) plot .

In FIG. 3 we show the normalized $T_c^*$-spectra for the DE magnetic amplitude with the E787 branching ratio [18] in TAB. II (upper plot) and the NA48/2 branching ratio in TAB. II (lower plot). The solid curves correspond to a constant amplitude, the dotted curves to a magnetic form factor with $\eta_V = 1.5$ and corresponding value of $A^+$ on the central (lower) full line of FIG. 2 for the upper (lower) plot.

Then we plot the $W$-spectra with $T_c^* \in [55, 90]$ MeV in FIG. 4 and $T_c^* \in [0, 80]$ MeV in FIG. 5. In each case we consider form factors with $\eta_V = 0.5$ (dashed curves) and $\eta_V = 1.5$ (dotted curves); the corresponding values of $A^+$ are determined from FIG.2.

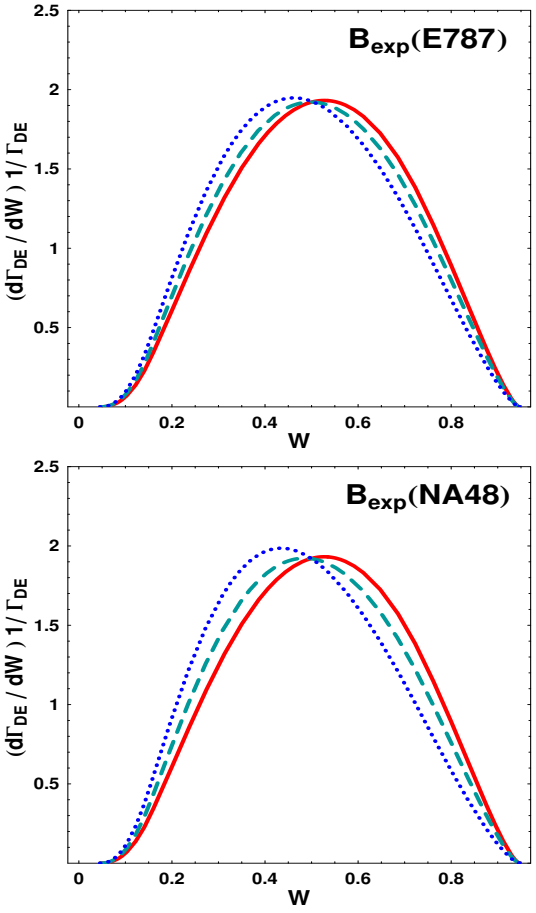


FIG. 4: Normalized $W$-spectra ($T_c^* \in [55, 90]$ MeV) for the DE magnetic amplitude. The upper and lower figures correspond to the E787 branching ratio [18] in TAB. II (the central solid line of FIG. 2) and to the NA48/2 branching ratio in TAB. II (the lower solid line of FIG. 2) respectively. The solid curves corresponds to a constant amplitude, while the dashed and dotted curves correspond to form factors with $\eta_V = 0.5$ and $\eta_V = 1.5$ respectively.

As we can see the changing of the value of the branching ratio generates a substantial effect in the $W-$spectra in FIGS. 5 and 6.

Subtracting the IB contribution to the $W$-spectrum in (8) and assuming $E$ and $M$ constant

one obtains

$$\frac{d\Gamma(E,M)}{dW} \propto INT(E)\ W^2 + DE(E,M)\ W^4. \quad (20)$$

Then we can fit this to the experimental data determining $E$ from the interference term, $INT(E)$, and $M$ from $DE(E,M)$. Since $M_+^{\rm pole}(z_i)$ in (17) is obviously not constant, we would like to question whether the presence of this form factor (and no interference), could simulate an interference term in (20) as observed by NA48/2 [12, 13]. In fact we plot in FIG.6 the difference among normalized W-spectra :

$$\Delta = \frac{1}{\mathcal{N}_{ff}}\frac{d\Gamma(0,M_+(z_i))}{dW} - \frac{1}{\mathcal{N}_{\rm const.}}\frac{d\Gamma(0,M_+^{\rm const.})}{dW} \quad (21)$$

where the first distribution is generated by the form factor structure in eq. (16) and the second one by constant magnetic term. We study this difference in FIG.6 for DE amplitudes corresponding to form factors with $\eta_V = 0.5$ (dashed line) and $\eta_V = 1.5$ (dotted line). $\mathcal{N}_{ff}$ and $\mathcal{N}_{\rm const.}$ are the normalization factors for W-spectra, corresponding to the form factor and constant magnetic term respectively.

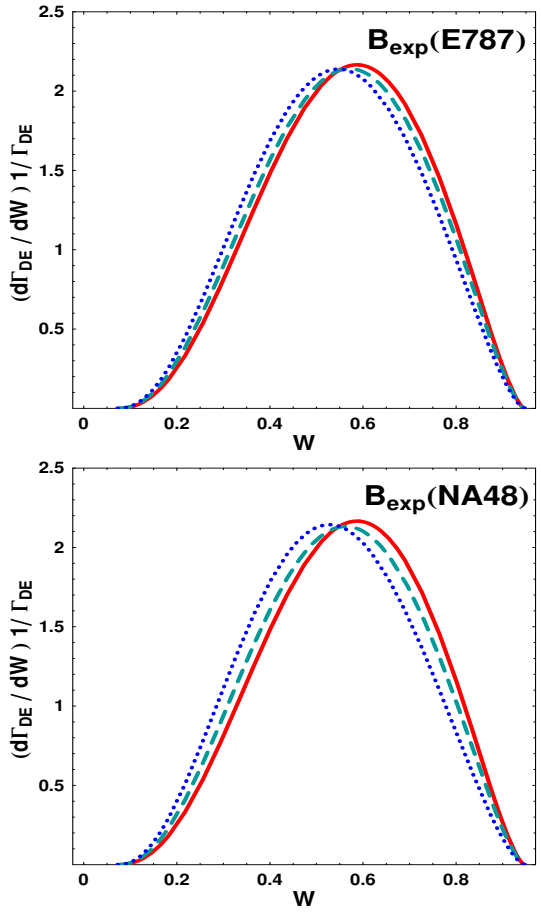


FIG. 5: Normalized $W$-spectra ($T_c^* \in [0, 80]$ MeV) for the DE magnetic amplitude. The upper and lower figures correspond to the E787 branching ratio [18] in TAB. II (the central solid line of FIG. 2) and to the NA48/2 branching ratio in TAB. II (the lower solid line of FIG. 2) respectively. The solid curves corresponds to a constant amplitude, while the dashed and dotted curves correspond to form factors with $\eta_V = 0.5$ and $\eta_V = 1.5$ respectively.

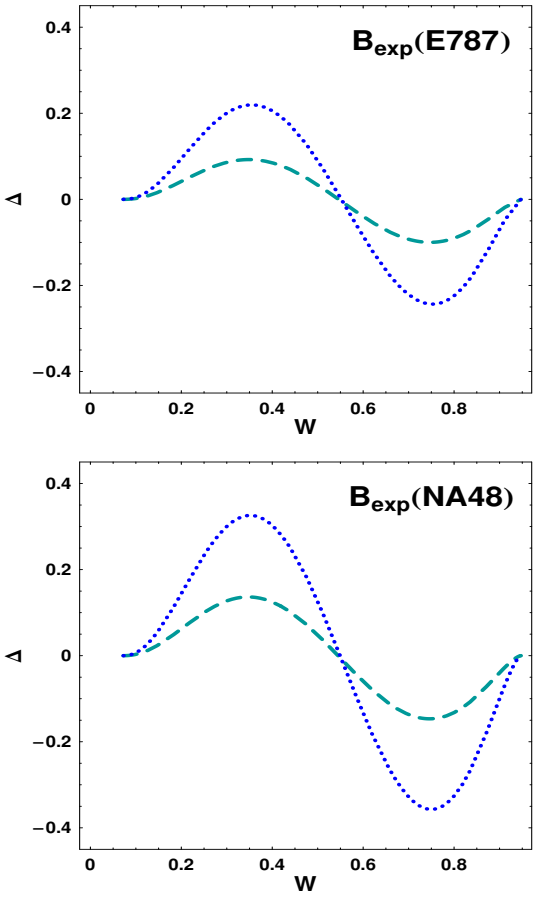


FIG. 6: Plots for the quantity $\Delta$ in eq. (21), obtained by subtracting the normalized $W$-spectrum of constant DE amplitude from the normalized $W$-spectra of DE amplitude corresponding to form factors with $\eta_V = 0.5$ (dashed line) and $\eta_V = 1.5$ (dotted line); upper and lower plots refer to E787 branching ratio [18] in TAB. II (the central solid line of FIG. 2) and to the NA48/2 branching ratio in TAB. II respectively (the lower solid line of FIG. 2). $T_c^*$-range is $[0, 80]$ MeV.

An interference term would appear as a line start-

ing from the origin and going to negative values for negative interference. It is clear that there is a correlation between the measurement of the interference and direct emissiom with form factor. We can see from FIG.6 that this depends also on the size of the branching ratio: the effect is $\leq 20\%$ for the E787 branching ratio and even 30% for the NA48/2 branching ratio in TAB. II and for the extreme value of the VMD parameter, $\eta_V = 1.5$ (dotted line). However we can exclude that the form factor can completely account for the interference effect.

## V. CONCLUSIONS

VMD has played a very crucial role for our understandings of chiral dynamics and its predictive power in the strong sector; we expect a similar success in the weak sector, however the path is apparentely more complicated. The magnetic contribution to $K_L \to \pi^+\pi^-\gamma$ decays is one of the few examples in the weak sector where there is phenomenological evidence of VMD. This is particularly interesting for the interplay with CP violating amplitudes and possible New Physics searches. Furthermore, the precision level of CPT tests is such that even $A(K_L \to \pi^+\pi^-\gamma)_{DE}$ has to be known with good accuracy [29].

We have studied in this paper the correlated channel $K^+ \to \pi^+\pi^0\gamma$, in connection with the upcoming NA48/2 results. We have analyzed in Section II a set of kinematical variables, Christ's variables, used also by NA48/2.

We have numerically analyzed how to find experimental evidence of VMD in this channel; compared to previous literature [16] we have payed particular attention to the dependence of the parameter $\eta_V$ and $A^+$, entering in this study, on the measured $B(K^+ \to \pi^+\pi^0\gamma)$ (see FIG. 2). After this analysis we have concentrated on the dependence of the spectra on VMD see FIGS. 3-5.

We have explored also the possible dependence of the observed interference effect, due to electric transitions, on the presence of a form factor in magnetic transitions. Since electric transitions are important from a chiral dynamics point of view this question is relevant: we have found that *i)* there is a correlation between the size of the branching ratio and the shape of the spectra and *ii)* for an accurate determination of the interference contribution the size of the form factor is relevant.

## ACKNOWLEDGEMENTS

This work has been supported in part by the European Commission (EC) RTN FLAVIAnet under Contract No. MRTN-CT-2006-035482 and by the Italian Ministry of Education and Research (MIUR), project 2005-023102. We thank Gino Isidori, Donald Cundy, Mauro Raggi and Marco Sozzi for continuous discussions and help.

[1] G. D'Ambrosio and G. Isidori, Int. J. Mod. Phys. A **13**, 1 (1998). [arXiv:hep-ph/9611284].
[2] S. Peris, M. Perrottet,and E. de Rafael, JHEP **9805**, 011 (1998); M.Knecht, S. Peris, and E. de Rafael, Phys. Lett. B **443**, 255 (1998); Phys. Lett. B **457**, 227 (1999); Nucl. Phys. Proc. Suppl. **86**, 279 (2000).
[3] G. Buchalla, A. J. Buras, and M. E. Lautenbacher, Rev. Mod. Phys. **68**, 1125 (1996).
[4] G. Ecker, H. Neufeld, A. Pich, Nucl. Phys. **B314**, 321(1994)
[5] G. D'Ambrosio and J. Portoles, Nucl. Phys. B **533** (1998) 523 [arXiv:hep-ph/9711210].
[6] A. R. Barker and S. H. Kettell, Ann. Rev. Nucl. Part. Sci. **50** (2000) 249 [arXiv:hep-ex/0009024].
[7] M. S. Sozzi and I. Mannelli, Riv. Nuovo Cim. **26**, 1 (2003) [arXiv:hep-ex/0312015].
[8] C. O. Dib and R. D. Peccei, Phys. Lett. B **249**, 325 (1990); Riazuddin, N. Paver and F. Simeoni, Phys. Lett. B **316**, 397 (1993) [arXiv:hep-ph/9308328]; G. Colangelo, G. Isidori and J. Portoles, Phys. Lett. B **470**, 134 (1999) [arXiv:hep-ph/9908415]; J. Tandean and G. Valencia, Phys. Rev. D **62**, 116007 (2000) [arXiv:hep-ph/0008238].
[9] G. D'Ambrosio, M. Miragliuolo and P. Santorelli, LNF-92-066-P *In *Maiani, L. (ed.) et al.: The DAPHNE physics handbook, vol. 1* 231-279*
[10] A. Alavi-Harati *et al.* [The KTeV Collaboration], Phys. Rev. Lett. **86** (2001) 761 [arXiv:hep-ex/0008045]. E. Abouzaid *et al.* [KTeV Collaboration], Phys. Rev. D **74** (2006) 032004 [Erratum-ibid. D **74** (2006) 039905].
[11] W.-M. Yao et al., J. Phys. G 33, 1 (2006)
[12] NA48/2 Coll., http://na48.web.cern.ch/NA48/NA48-2/NA48_2.html
[13] M. Raggi and D. Cundy: private comunications; M. Raggi, talk at BEACH 2006, http://www.hep.lancs.ac.uk/Beach2006/
[14] G. Ecker, J. Kambor, and D. Wyler, Nucl. Phys. **B394**, 101(1993).
[15] G. D'Ambrosio and J. Portoles, *Nucl. Phys.* **B 533** (1998) 494 [hep-ph/9711211].
[16] G. D'Ambrosio and D. N. Gao, JHEP **0010**, 043 (2000) [arXiv:hep-ph/0010122].
[17] N. Christ, Phys. Rev. **159** (1967) 1292.
[18] S. C. Adler *et al.* [E787 Collaboration], Phys. Rev.

Lett. **85**, 4856 (2000) [arXiv:hep-ex/0007021].
[19] M. A. Aliev *et al.* [KEK-E470 Collaboration], Phys. Lett. B **554**, 7 (2003) [arXiv:hep-ex/0212048]. V. A. Uvarov *et al.*, Phys. Atom. Nucl. **69**, 26 (2006) [arXiv:hep-ex/0410049]. M. A. Aliev *et al.* [KEK-E470 Collaboration], Eur. Phys. J. C **46**, 61 (2006) [arXiv:hep-ex/0511060].
[20] G. D'Ambrosio and G. Isidori, Z. Phys. **C65**,649 (1995); [arXiv:hep-ph/9408219].
[21] G. D'Ambrosio, G. Ecker, G. Isidori, and H. Neufeld, *Radiative non-leptonic kaon decays*, in The Second DAΦNE physics Handbook, ed. L. Maiani, G. Pancheri and N. Paver, LNF (1995) p. 265. arXiv:hep-ph/9411439.
[22] C. Bruno and J. Prades, Z. Phys. C **57**, 585 (1993) [arXiv:hep-ph/9209231].
[23] G. D'Ambrosio, M. Miragliuolo, and F. Sannino, Z. Phys. **C59**, 451 (1993).
[24] H. Taureg *et al.*, Phys. Lett. B **65** (1976) 92.
[25] J. Bijnens, G. Ecker and A. Pich, Phys. Lett. B **286**, 341 (1992) [arXiv:hep-ph/9205210].
[26] A. Lai *et al.* [NA48 Collaboration], Eur. Phys. J. C **30** (2003) 33.
[27] E. Abouzaid *et al.* [KTeV Collaboration], Phys. Rev. Lett. **96** (2006) 101801 [arXiv:hep-ex/0508010].
[28] G. Ecker, A. Pich and E. de Rafael, Phys. Lett. B **237**, 481 (1990).
[29] F. Ambrosino *et al.* [KLOE Collaboration], JHEP **0612**, 011 (2006) [arXiv:hep-ex/0610034].